Genomics Proteomics Bioinformatics 11 (2013) 320–326

Genomics Proteomics Bioinformatics

www.elsevier.com/locate/gpb
www.sciencedirect.com

ORIGINAL RESEARCH

Induced Pluripotent Stem Cells Are Sensitive to DNA Damage

Minjie Zhang, Caiyun Yang, Huixian Liu, Yingli Sun *

Beijing Institute of Genomics, Chinese Academy of Sciences, Beijing 100101, China

Received 22 July 2013; revised 28 August 2013; accepted 3 September 2013
Available online 4 October 2013

KEYWORDS

iPSCs;
MEF cells;
γ-H2AX;
DNA damage;
Whole-genome sequencing

Abstract Induced pluripotent stem cells (iPSCs) resemble embryonic stem cells (ESCs) in morphology, gene expression and *in vitro* differentiation, raising new hope for personalized clinical therapy. While many efforts have been made to improve reprogramming efficiency, significant problems such as genomic instability of iPSCs need to be addressed before clinical therapy. In this study, we try to figure out the real genomic state of iPSCs and their DNA damage response to ionizing radiation (IR). We found that iPSC line 3FB4-1 had lower DNA damage repair ability than mouse embryonic fibroblast (MEF) cells, from which 3FB4-1line was derived. After the introduction of DNA damage by IR, the number of γ-H2AX foci in 3FB4-1 increased modestly compared to a large increase seen in MEF, albeit both significantly ($P < 0.01$). In addition, whole-genome sequencing analysis showed that after IR, 3FB4-1 possessed more point mutations than MEF and the point mutations spread all over chromosomes. These observations provide evidence that iPSCs are more sensitive to ionizing radiation and their relatively low DNA damage repair capacity may account for their high radiosensitivity. The compromised DNA damage repair capacity of iPSCs should be considered when used in clinical therapy.

Introduction

Embryonic stem cells (ESCs) maintain pluripotency and are capable of differentiating into all somatic cell types, which thus may be used to treat some diseases [1]. However, the clinical applications of ESCs have been limited due to the ethical concerns. In 2006, Yamanaka and his team successfully obtained ESC-like pluripotent stem cells, termed induced pluripotent stem cells (iPSCs), through the introduction of four transcription factors (*Oct4*, *Sox2*, *c-Myc* and *Klf4*) into mouse somatic cells. The generated iPSCs are similar to ESCs in terms of morphology, gene expression, epigenetic status and *in vitro* differentiation capability [2]. Recent studies have been focused on the development of techniques for enhancing reprogramming efficiency, such as retrovirus-mediated introduction of transcription factors, lentiviral transduction, adenoviral infection, transient plasmid delivery, protein transduction system, and mRNA-mediated introduction [3–8]. However, evidence shows that genomic instability arises in generated iPSCs, which would affect their clinical applications [9–12].

Currently the genome of iPSCs is being scrutinized, and recent work shows that iPSCs contain chromosomal

* Corresponding author.
E-mail: sunyl@big.ac.cn (Sun Y).

Peer review under responsibility of Beijing Institute of Genomics, Chinese Academy of Sciences and Genetics Society of China.

Production and hosting by Elsevier

http://dx.doi.org/10.1016/j.gpb.2013.09.006

aberrations, such as chromosome 12 duplications in human iPSCs [13] and aberrantly silenced genes on chromosome 12qF1 in mouse iPSCs [11]. In addition, the reprogramming process in iPSCs is often incomplete because donor cells influence iPSCs in both transcriptional and epigenetic properties [9,10,12,14,15]. The level of copy number variations (CNVs) also increases in the early-passage iPSC lines, and most of the *de novo* CNVs result from the replication stress during the reprogramming process [16,17]. Another study shows that the absence of p53 increases the efficiency of reprogramming. However, it also raises the possibility of DNA damage and genomic instability accompanying the reprogramming process [18]. These findings suggest that iPSCs are more likely to harbor genomic abnormalities. Therefore, more attention should be paid to the genomic status of iPSCs before they are used in clinical therapy [19].

We introduced DNA damage through ionizing radiation (IR) to investigate whether the difference in DNA damage repair capacity of iPSCs, compared to mouse embryonic fibroblast (MEF) cells, is responsible for the genomic instability. Our results show that iPSC line 3FB4-1 is more sensitive to DNA damage due to their lower DNA damage repair ability. These findings would provide a novel insight into the genome instability of iPSCs.

Results

iPSCs display low DNA damage repair ability after IR

Previous studies demonstrated that DNA repair mechanisms play an important role in maintaining genomic stability [20–23]. We hypothesized that the genome instability of iPSCs is due to low DNA damage repair ability. To test this hypothesis, we treated mouse iPSC line 3FB4-1 and somatic MEF cells, from which 3FB4-1line was derived, with IR. IR can result in double strand breaks (DSBs), which are the most detrimental DNA lesions [24–26]. DSBs occur during the programmed genome rearrangement process and normal cell metabolism, and can cause genome abnormalities, apoptosis and senescence, if not repaired properly [27]. Our pilot time-course studies indicated that DNA damage response was evident 4 h after treatment with IR at 4 grays (data not shown). Immunoblotting analysis showed that ataxia-telangiectasia-mutated (ATM), which is essential for the initiation of DNA repair [28], underwent auto-phosphorylation and became activated after IR (**Figure 1A** and **B**). In addition, levels of γ-H2AX, the phosphorylated form of histone variant H2AX, which is a DSB marker, were differentially altered between 3FB4-1 and MEF. For 3FB4-1, the number of γ-H2AX foci per nucleus significantly increased in cells treated with IR at 4 grays (Gy), compared to the untreated controls (12 ± 0.7 vs 8 ± 1, $P < 0.01$). Significant increase in the number of γ-H2AX focus was also observed for the MEF cells treated with the same dosage of IR in comparison with the control cells. However, a much greater fold of increase was revealed for the MEF cells (20 ± 0.6 vs 1 ± 0.5, $P < 0.01$) (**Figure 1C–E**). The relatively modest increase in the number of γ-H2AX focus for iPSC line 3FB4-1 suggests that compared to MEF cells, iPSCs may have a low DNA damage repair capacity and that they are likely more sensitive to DNA damage.

Whole-genome sequencing of iPSCs and MEFs

To further evaluate the outcomes of differential DNA damage repair ability, we performed whole-genome DNA sequencing and single nucleotide variation (SNV) analysis for 3FB4-1 and MEF cells with (IR+) or without IR (IR−) treatment. 3FB4-1 cells were collected through the gelatin re-suspension method to eliminate the possible contamination of feeder cells. For all four samples, more than 6.3×10^8 reads per sample were generated and analyzed (**Table 1**). We obtained DNA sequences of >64 Gb per sample, and the amount of sequence data covered 25-fold and higher of each genome. Therefore, we were confident to detect true mutations for each sample.

SNV analysis reveals more point mutations present in iPSCs after IR

We used Burrows–Wheeler Alignment tool (BWA) [29] and Samtools Sequence Alignment/Map tool [30] to map the mouse reference genome sequence (mm9), and used VarScan [31] to call total SNVs for each sample. Approximately 2.9–4.2×10^6 SNVs were detected in each sample (Table 1). When sequence variation was directly compared between 3FB4-1 (IR−) and 3FB4-1 (IR+), or MEF (IR−) and MEF (IR+), about 908,296 likely SNVs were found in 3FB4-1 after IR, whereas only 183,518 SNVs were found in MEF (Table 1).

To further investigate the functions of SNVs indentified in 3FB4-1 and MEF after IR, we focused on SNVs that were not present in the dbSNP database (SNP128, downloaded from UCSC). By filtering the single nucleotide polymorphisms (SNPs) available in dbSNP, we identified the point mutations for each sample (Table 1). Results showed that compared to non-treated counterpart, the number of mutations for 3FB4-1 cells increased sharply after IR, from 494,616 to 936,728, whereas the number of mutations barely increased for MEF cells, from 1,243,249 to 1,312,621 (Table 1 and **Figure 2**). In 3FB4-1 cells, 302,226 SNVs were commonly found in both 3FB4-1 (IR−) and 3FB4-1 (IR+) cells, whereas 634,502 SNVs were uniquely recovered from 3FB4-1 (IR+) cells. Conversely, 327,625 SNVs were uniquely recovered from MEF (IR+), while MEF (IR−) and MEF (IR+) shared more common SNVs (984,996 SNVs). These data indicated that more IR-induced SNVs were present in 3FB4-1 cells than in MEF cells.

Next, we examined the chromosomal distribution of the IR-induced point mutations in 3FB4-1 and MEF. Our analysis indicated that point mutations spread all over chromosomes. And no enrichment of point mutations was observed in any specific chromosomes. For 3FB4-1 cells, the number of point mutations increased markedly in each chromosome (**Figure 3A**, Table S1). However, compared to non-irradiated controls, number of point mutations increased approximately 3–6% in each chromosome for MEF cells after IR (**Figure 3B**, Table S1). For example, on Chromosome 10, the number of mutations increased 356% in 3FB4-1 cells, but only 4.91% in MEF cells after IR (Table S1).

Point mutations in known functional elements of the genome

The point mutations found in the 3FB4-1 and MEF cells after IR were further classified to identify functional relevance.

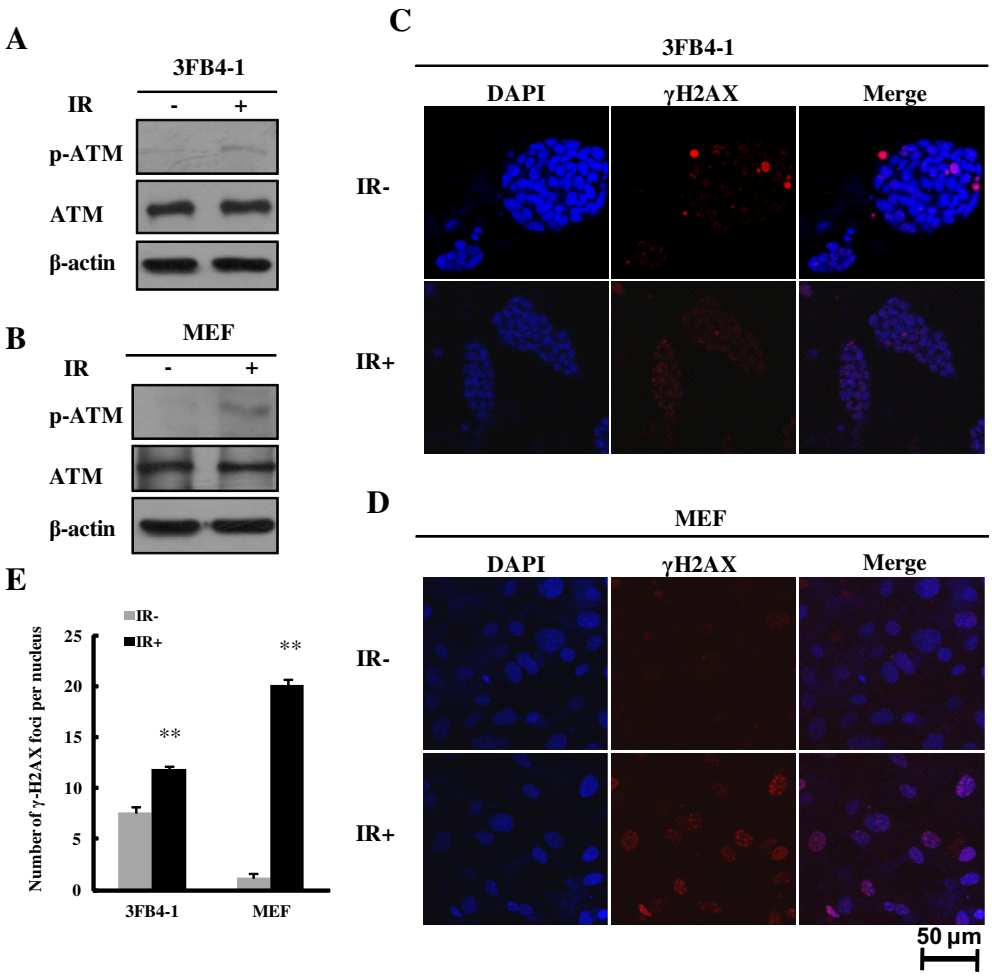

Figure 1 IR induced DNA damage response in 3FB4-1 and MEF cells

A–**B**. Western blot analysis of phosphorylated ATM and total ATM for 3FB4–1 (**A**) and MEF (**B**) with (IR+) or without (IR−) 4 Gy of IR. β-Actin serves as the loading control. **C**–**D**. Representative γ-H2AX focus images are shown for 3FB4-1 (**C**) and MEF (**D**) with or without IR. Red, γ-H2AX; Blue, DAPI (for DNA). **E**. Quantification for the numbers of γ-H2AX focus in 3FB4-1 and MEF cells. Error bars represent the standard error of the mean (SEM) for the numbers of γ-H2AX foci per nucleus based on 4–5 fields with approximately 20–30 cells per field; $^{**}P < 0.01$.

Table 1 Summary of sequencing results for 3FB4-1 and MEF genomes

Feature	3FB4-1		MEF	
	IR−	IR+	IR−	IR+
Total nucleotides sequenced	64.1 Gb	71.5 Gb	64.7 Gb	70.1 Gb
Genome coverage (fold)	25×	28×	25×	28×
Total number of reads	634,852,868	708,065,514	640,447,936	693,376,402
Total number of SNVs	2,906,794	3,815,090	4,030,205	4,213,723
Total number of point mutations	494,616	936,728	1,243,249	1,312,621

Note: SNV stands for single nucleotide variation.

Results showed that most of these point mutations resided within intergenic regions and introns (Figure 4). In addition, there were a few point mutations found in the 5′ untranslated regions (5′UTRs) and 3′UTRs, and several in the splice site (2-nt near exon boundary) (Figure 4, Table S2). Next, we focused on point mutations in coding regions especially. Compared to non-irradiated cells, there were 2256 and 949 synonymous point mutations in 3FB4-1 and in MEF, respectively, after IR. Additionally, 1454 and 724 nonsynonymous point mutations were revealed in IR-treated 3FB4-1 and MEF, respectively. However, the number of nonsense mutations in the coding regions was comparable for 3FB4-1 and MEF after IR. These results indicated that the remarkable changes in irradiated 3FB4-1, which are consistent with our finding that iPSCs have lower DNA damage repair ability and are more sensitive to DNA damage.

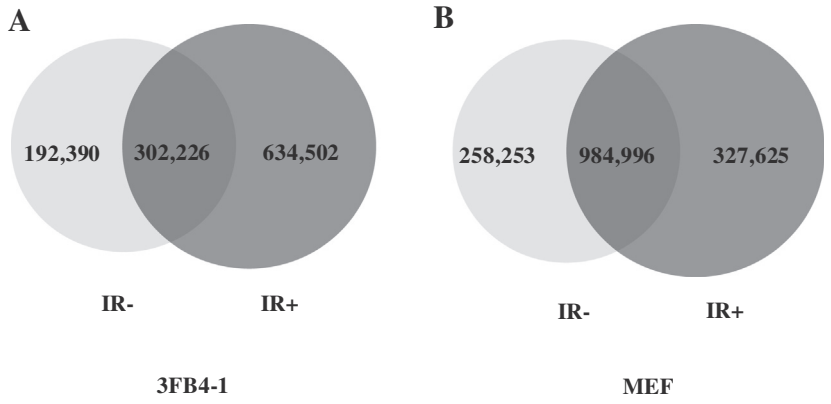

Figure 2 Venn diagram for point mutations in the 3FB4-1 and MEF genomes
The number of point mutations is shown for 3FB4-1 (**A**) and MEF (**B**) with or without IR.

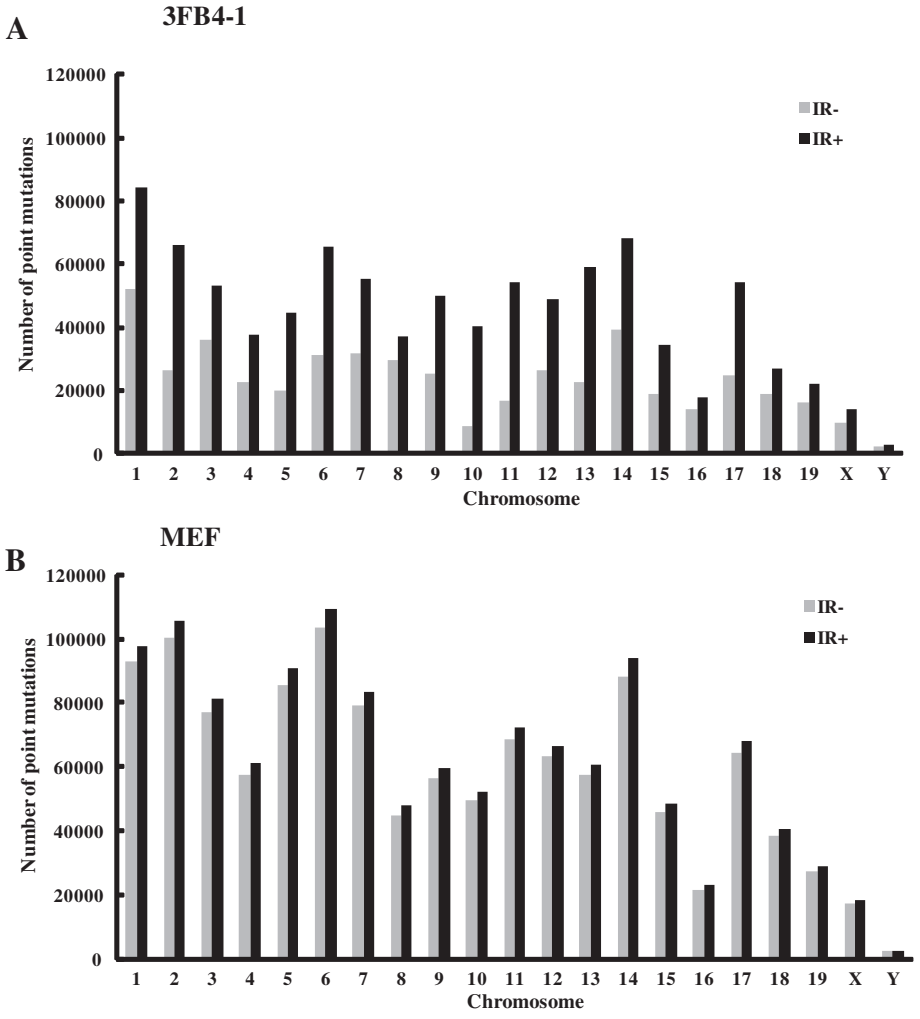

Figure 3 Chromosomal distribution of point mutations
The number of point mutations in each chromosome is shown for 3FB4-1 (**A**) and MEF (**B**) with or without IR.

Discussion

Previous research has focused on the reprogramming processes to improve the efficiency of iPSCs generation. However, less attention has been paid to the genomic status of iPSCs [32–34]. Recently, several studies reported that iPSCs are more likely to harbor genomic abnormalities [35,36] and the observed genomic aberrations may result from the reprogramming process [16,37]. DNA repair mechanisms are essential for maintaining genomic stability of cells as well [20–23].

To test whether the altered DNA repair ability is responsible for genomic instability of iPSCs, we introduced DSBs to somatic cell line MEF, iPSC line 3FB4-1derived from MEF and ESC line E14 through IR. By immunofluorescence and immunoblotting analysis, we found that 3FB4-1 had more γ-H2AX foci than E14 and MEF, even without irradiation (current study and data not shown). However, 3FB4-1 had a relative low increase in the number of γ-H2AX focus compared to E14 and MEF after IR (current study and data not shown). In the present study, we compared MEF and 3FB4-1 in terms of DNA damage response. The results accumulated in this study suggest that iPSCs were more sensitive to IR due to their low DNA damage repair ability.

In normal situations, iPSCs could accurately repair DSBs mostly through the homologous recombination (HR) pathway [38]. Somatic cells mostly adopt the error prone non-homologous end joining (NHEJ) pathway to repair DNA damage [39]. This difference in repair mechanism may explain the lower basal mutation rate in 3FB4-1 compared to MEF. However, when DSBs were introduced by IR, 3FB4-1 showed higher sensitivity to DNA damage than MEF, which may be one important indicator of genomic instability for iPSCs. Therefore, likely, we could improve the genomic stability of iPSCs through regulation of the DNA damage repair response to reduce the risk of tumor formation prior to use in clinical therapy. However, further studies would be necessary to identify genes that are mutated during IR and to eventually find the mechanism underlying the sensitivity of iPSCs to DNA damage, which could be approached, for example, by comparing the DNA repair capability of more cell types including iPSCs, ESCs and other somatic cells.

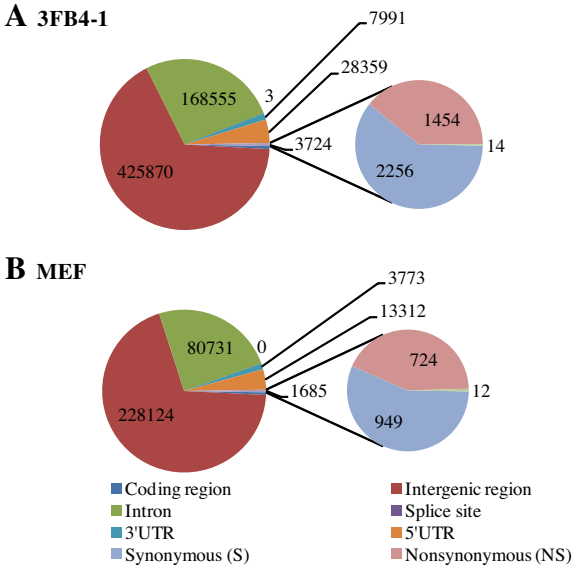

Figure 4 Distribution of IR-induced point mutations in known functional elements

The IR-induced point mutations in 3FB4-1 (**A**) and MEF (**B**) genome were analyzed according to known functional elements: intergenic regions, introns, 5′UTRs, 3′UTRs, splice site and coding regions; the point mutations residing within coding regions were further analyzed based on variant type: synonymous, nonsynonymous and nonsense.

Materials and methods

Cell lines and cell culture

Mouse iPSC line 3FB4-1 was cultured in Dulbecoo's Modified Eagle Medium (DMEM, Gibco, Grand Island, New York, USA) supplemented with 15% Embryonic Stem Cell Fetal Bovine Serum (ES Cell FBS; Gibco, New Zealand), 1% MEM Non-Essential Amino Acids (MEM NEAA; Grand Island, New York, USA), 1% penicillin/streptomycin (Gibco, Grand Island, New York, USA), 2 mM L-glutamine solution (Gibco, Grand Island, New York, USA), 10^3 units/ml medium Mouse Leukemia Inhibitory Factor (LIF; Millopore, Temecula, CA, USA), 0.1 mM 2-mercaptoethanol (Gibco, Grand Island, New York, USA) [40]. Medium was changed daily and the iPSCs were passaged every two days using Trypsin 0.25% Solution (Thermo Fisher Scientific, Beijing, China). MEF cells were cultured in DMEM (Thermo Fisher Scientific, Beijing, China) supplemented with 15% FBS (Thermo Fisher Scientific, Beijing, China) and 1% NEAA, 1% penicillin/streptomycin [41].

Irradiation

Cells were passaged one day before IR and were irradiated with 4 Gy of γ-irradiation using a cobalt irradiator. After IR, cells were returned to the incubator immediately and cultured for 4 more hours before further analysis.

Western blotting analysis

Cells were lysed in ATM lysis buffer (20 mM HEPES, pH 7.4, 150 mM NaCl, 0.2% Tween 20, 1.5 mM $MgCl_2$, 1 mM EGTA, 2 mM dithiothreitol, 50 mM NaF, 500 μM $NaVO_4$, 1 mM phenylmethylsulfonyl fluoride, 0.1 μg/ml aprotinin and 0.1 μg/ml leupeptin) and cleared by centrifugation [42]. Proteins were separated by SDS–PAGE and transferred to PVDF membranes (Millipore, Billerica, MA, USA). The blots were incubated with primary antibodies against p-ATM (1:1000, R&D Systems, MN, USA), ATM (1:3000; Gene Tex, San Diego, CA, USA), β-actin (1:3000, Beyotime Biotech). After washing in 1× PBS three times, blots were incubated with an anti mouse secondary antibody conjugated with HRP (1:3000; Gene Tex, San Diego, CA, USA) and anti rabbit secondary antibody conjugated with HRP (1:3000; Abcam, Cambridge, MA, USA), respectively. Finally, blots were washed and bands were visualized by the Image Quant ECL equipment (GE healthcare, Piscataway, NJ, USA).

γH2AX immunofluoresence

Cells were passaged on slides one day before IR. After exposure to 0 or 4 Gy of γ-irradiation, cells were put back into the incubator at 37 °C. Four hours later, cells were washed in phosphate-buffered saline (PBS) and fixed with 4% paraformaldehyde for 10 min at room temperature. After washing with PBS, cells were permeabilized for 10 min in 0.05% Triton X-100 and 0.5% NP-40, followed by washing in PBS for 3 times (5 min each). Slides with cells were blocked with 2%

BSA for 1 h and then incubated with mouse anti-γH2AX antibody (1:500; Millipore, CA, USA) for 1 h at room temperature. After washing with PBS containing 0.05% Tween 20 for three times, the goat anti-mouse secondary antibody (1:800, Abcam, Cambridge, MA, USA) was applied for incubation for 1 h in the dark at room temperature, at the same time, slides were stained with 0.2 mg/ml of 4′,6-diamidino-2-phenylindole (DAPI, 1:2000; Sigma, Shanghai, China). Confocal images were acquired and analyzed on Leica TCS SP5 (Leica) equipped with HCX PL 63 × 1.4 oil CS immersion objective.

DNA extraction

iPSCs 3FB4-1 cells were digested using Trypsin 0.25% solution and resuspended in gelatin-coated dishes. After incubation at 37 °C for 10–30 min, the supernatant was transferred into a 15 ml centrifuge tube to collect the cell precipitate by centrifugation at 1000 rpm for 5 min at room temperature. Then DNA was extracted using QIAamp DNA Mini Kit (QIAGEN, Hilden, Germany) as instructed by the manufacturer.

Whole-genome sequencing

Whole genome DNA libraries suitable for sequencing on Illumina's sequencing platform were generated from 5 μg of genomic DNA. The DNA was sheared to approximately 300–500 bp with a Covaris S220 (Life Technologies, USA). The libraries were sequenced on HiSeq2000 DNA Sequencer (Illumina). In addition, to reduce the false positive errors in library preparations and sequencing process, we prepare the four samples in parallel and sequenced them within one flowcell (two lanes per sample).

SNV analysis

Sequencing data were mapped to mouse reference genome sequence (mm9) and SNVs were called using VarScan software (min-coverage 10, min-reads 2, min-avq-qual 20, min-var-freq 0.20, *P* value 0.99) [31]. The dbSNP database (SNP128) was downloaded from UCSC (http://genome.ucsc.edu/).

Authors' contributions

YS conceived the project and designed experiments. MZ, CY and HL collected the data. MZ performed the analysis. All authors read and approved the final manuscript.

Competing interests

The authors have no competing interests to declare.

Acknowledgements

This work was supported by Strategic Priority Research Program of the Chinese Academy of Sciences (Grant No. XDA01040405), National Natural Science Foundation of China (Grant No. 91029024) and National Basic Research Program of China (973 Program; Grant No. 2013CB911001).

Supplementary material

Supplementary data associated with this article can be found, in the online version, at http://dx.doi.org/10.1016/j.gpb.2013.09.006.

References

[1] Thomson JA, Itskovitz-Eldor J, Shapiro SS, Waknitz MA, Swiergiel JJ, Marshall VS, et al. Embryonic stem cell lines derived from human blastocysts. Science 1998;282:1145–7.
[2] Takahashi K, Yamanaka S. Induction of pluripotent stem cells from mouse embryonic and adult fibroblast cultures by defined factors. Cell 2006;126:663–76.
[3] Takahashi K, Tanabe K, Ohnuki M, Narita M, Ichisaka T, Tomoda K, et al. Induction of pluripotent stem cells from adult human fibroblasts by defined factors. Cell 2007;131:861–72.
[4] Brambrink T, Foreman R, Welstead GG, Lengner CJ, Wernig M, Suh H, et al. Sequential expression of pluripotency markers during direct reprogramming of mouse somatic cells. Cell Stem Cell 2008;2:151–9.
[5] Zhou W, Freed CR. Adenoviral gene delivery can reprogram human fibroblasts to induced pluripotent stem cells. Stem Cells 2009;27:2667–74.
[6] Okita K, Nakagawa M, Hyenjong H, Ichisaka T, Yamanaka S. Generation of mouse induced pluripotent stem cells without viral vectors. Science 2008;322:949–53.
[7] Zhou H, Wu S, Joo JY, Zhu S, Han DW, Lin T, et al. Generation of induced pluripotent stem cells using recombinant proteins. Cell Stem Cell 2009;4:381–4.
[8] Warren L, Manos PD, Ahfeldt T, Loh Y-H, Li H, Lau F, et al. Highly efficient reprogramming to pluripotency and directed differentiation of human cells with synthetic modified mRNA. Cell Stem Cell 2010;7:618–30.
[9] Kim K, Doi A, Wen B, Ng K, Zhao R, Cahan P, et al. Epigenetic memory in induced pluripotent stem cells. Nature 2010;467:285–90.
[10] Lister R, Pelizzola M, Kida YS, Hawkins RD, Nery JR, Hon G, et al. Hotspots of aberrant epigenomic reprogramming in human induced pluripotent stem cells. Nature 2011;471:68–73.
[11] Stadtfeld M, Apostolou E, Akutsu H, Fukuda A, Follett P, Natesan S, et al. Aberrant silencing of imprinted genes on chromosome 12qF1 in mouse induced pluripotent stem cells. Nature 2010;465:175–81.
[12] Kim K, Zhao R, Doi A, Ng K, Unternaehrer J, Cahan P, et al. Donor cell type can influence the epigenome and differentiation potential of human induced pluripotent stem cells. Nat Biotechnol 2011;29:1117–9.
[13] Mayshar Y, Ben-David U, Lavon N, Biancotti JC, Yakir B, Clark AT, et al. Identification and classification of chromosomal aberrations in human induced pluripotent stem cells. Cell Stem Cell 2010;7:521–31.
[14] Polo JM, Liu S, Figueroa ME, Kulalert W, Eminli S, Tan KY, et al. Cell type of origin influences the molecular and functional properties of mouse induced pluripotent stem cells. Nat Biotechnol 2010;28:848–55.
[15] Bar-Nur O, Russ HA, Efrat S, Benvenisty N. Epigenetic memory and preferential lineage-specific differentiation in induced pluripotent stem cells derived from human pancreatic islet beta cells. Cell Stem Cell 2011;9:17–23.
[16] Hussein SM, Batada NN, Vuoristo S, Ching RW, Autio R, Narva E, et al. Copy number variation and selection during reprogramming to pluripotency. Nature 2011;471:58–62.
[17] Laurent LC, Ulitsky I, Slavin I, Tran H, Schork A, Morey R, et al. Dynamic changes in the copy number of pluripotency and

cell proliferation genes in human ESCs and iPSCs during reprogramming and time in culture. Cell Stem Cell 2011;8:106–18.
[18] Marion RM, Strati K, Li H, Murga M, Blanco R, Ortega S, et al. A p53-mediated DNA damage response limits reprogramming to ensure iPS cell genomic integrity. Nature 2009;460:1149–53.
[19] Gore A, Li Z, Fung HL, Young JE, Agarwal S, Antosiewicz-Bourget J, et al. Somatic coding mutations in human induced pluripotent stem cells. Nature 2011;471:63–7.
[20] Rooney S, Alt FW, Lombard D, Whitlow S, Eckersdorff M, Fleming J, et al. Defective DNA repair and increased genomic instability in Artemis-deficient murine cells. J Exp Med 2003;197:553–65.
[21] Zha S, Alt FW, Cheng HL, Brush JW, Li G. Defective DNA repair and increased genomic instability in Cernunnos-XLF-deficient murine ES cells. Proc Natl Acad Sci U S A 2007;104:4518–23.
[22] Lombard DB, Chua KF, Mostoslavsky R, Franco S, Gostissa M, Alt FW. DNA repair, genome stability, and aging. Cell 2005;120:497–512.
[23] Kalra RS, Bapat SA. Enhanced levels of double-strand DNA break repair proteins protect ovarian cancer cells against genotoxic stress-induced apoptosis. J Ovarian Res 2013;6:66.
[24] Khanna KK, Jackson SP. DNA double-strand breaks: signaling, repair and the cancer connection. Nat Genet 2001;27:247–54.
[25] Shrivastav M, De Haro LP, Nickoloff JA. Regulation of DNA double-strand break repair pathway choice. Cell Res 2008;18:134–47.
[26] Jackson SP. Sensing and repairing DNA double-strand breaks. Carcinogenesis 2002;23:687–96.
[27] Cahill D, Connor B, Carney JP. Mechanisms of eukaryotic DNA double strand break repair. Front Biosci 2006;11:1958–76.
[28] Lavin MF, Birrell G, Chen P, Kozlov S, Scott S, Gueven N. ATM signaling and genomic stability in response to DNA damage. Mutat Res 2005;569:123–32.
[29] Li H, Durbin R. Fast and accurate short read alignment with Burrows–Wheeler transform. Bioinformatics 2009;25:1754–60.
[30] Li H, Handsaker B, Wysoker A, Fennell T, Ruan J, Homer N, et al. The Sequence Alignment/Map format and SAMtools. Bioinformatics 2009;25:2078–9.
[31] Koboldt DC, Zhang Q, Larson DE, Shen D, McLellan MD, Lin L, et al. VarScan 2: somatic mutation and copy number alteration discovery in cancer by exome sequencing. Genome Res 2012;22:568–76.
[32] Maherali N, Hochedlinger K. Guidelines and techniques for the generation of induced pluripotent stem cells. Cell Stem Cell 2008;3:595–605.
[33] Daley GQ, Lensch MW, Jaenisch R, Meissner A, Plath K, Yamanaka S. Broader implications of defining standards for the pluripotency of iPSCs. Cell Stem Cell 2009;4:200–1.
[34] Ellis J, Bruneau BG, Keller G, Lemischka IR, Nagy A, Rossant J, et al. Alternative induced pluripotent stem cell characterization criteria for in vitro applications. Cell Stem Cell 2009;4:198–9.
[35] Pasi CE, Dereli-Oz A, Negrini S, Friedli M, Fragola G, Lombardo A, et al. Genomic instability in induced stem cells. Cell Death Differ 2011;18:745–53.
[36] Ronen D, Benvenisty N. Genomic stability in reprogramming. Curr Opin Genet Dev 2012;22:444–9.
[37] Jiang J, Lv W, Ye X, Wang L, Zhang M, Yang H, et al. Zscan4 promotes genomic stability during reprogramming and dramatically improves the quality of iPS cells as demonstrated by tetraploid complementation. Cell Res 2013;23:92–106.
[38] Johnson RD, Jasin M. Double-strand-break-induced homologous recombination in mammalian cells. Biochem Soc Trans 2001;29:196–201.
[39] Lieber MR. The mechanism of human nonhomologous DNA end joining. J Biol Chem 2008;283:1–5.
[40] Esteban MA, Wang T, Qin BM, Yang JY, Qin DJ, Cai JL, et al. Vitamin C enhances the generation of mouse and human induced pluripotent stem cells. Cell Stem Cell 2010;6:71–9.
[41] Huangfu DW, Maehr R, Guo WJ, Eijkelenboom A, Snitow M, Chen AE, et al. Induction of pluripotent stem cells by defined factors is greatly improved by small-molecule compounds. Nat Biotechnol 2008;26:795–7.
[42] Sun Y, Xu Y, Roy K, Price BD. DNA damage-induced acetylation of lysine 3016 of ATM activates ATM kinase activity. Mol Cell Biol 2007;27:8502–9.